4

The Other Side of the Embryo: An Appreciation of the Non-D Quadrants in Leech Embryos

David A. Weisblat, Françoise Z. Huang, Deborah E. Isaksen, Nai-Jia L. Liu, and Paul Chang
Department of Molecular and Cell Biology
University of California
Berkeley, California 94720

I. Introduction and Overview of Leech Development

In animals that develop by spiral cleavages (including annelids, mollusks, and several other protostome taxa), the first two cleavage planes include or lie parallel to the animal/vegetal axis, generating four blastomeres designated as A, B, C, and D. A general feature of spiralian development is that one quadrant (widely designated as the D quadrant) contributes the bulk of the mesoderm to the embryo. Thus, studies on the mechanisms of cell fate determination in spiralian embryos have tended to focus on the question of how the D quadrant is determined to be different from the A, B, and C quadrants, either by the segregation of developmental determinants, for species in which initial cleavages are unequal, or by cell–cell interactions, for species in which initial cleavages are equal (Goldstein and Freeman, 1997; Freeman and Lundelius, 1992; Pilon and Weisblat, 1997; Boyer *et al.*, 1996). Analysis of segmentation in the leech as an example of embryonic pattern formation also focuses attention on the D quadrant deriva-

Current Topics in Developmental Biology, Vol. 46

0070-2153/99 $30.00

tives because the D quadrant is the precursor of segmental ectoderm and mesoderm (Wedeen, 1995; Savage and Shankland, 1997).

In contrast, the goal of this article is to summarize findings that reveal a phenomenologically rich developmental cell biology in the A, B, and C quadrants in embryos of glossiphoniid leeches, such as *Helobdella robusta* (class Hirudinea; phylum Annelida). In glossiphoniid leeches, these non-D quadrants are precursors of definitive endoderm (Whitman, 1878; Bychowsky, 1921; Nardelli-Haefliger and Shankland, 1993) among other tissues (Nardelli-Haefliger and Shankland, 1993; Smith and Weisblat, 1994; Huang *et al.*, 1999). To appreciate the roles of these cells in embryogenesis, however, it is necessary first to summarize glossiphoniid leech development in terms of the contributions of the D quadrant.

Leeches are examples of "unequal cleavers," in which factors influencing subsequent cell fates (i.e., determinants) are partitioned unequally during the first two cleavages; in such embryos, the second embryonic axis is therefore recognizable at first cleavage (with the first, animal/vegetal axis being recognizable upon the migration of the female pronucleus just prior to polar body formation). In the leech, some determinants are contained within animal and vegetal domains of yolk-free cytoplasm (teloplasm) that arise prior to first cleavage and are distributed unequally during the first two cleavages into the D quadrant (Fernandez and Olea, 1982; Astrow *et al.*, 1987; Nelson and Weisblat 1991, 1992).

The eight-cell *Helobdella* embryo exhibits an apparently typical spiralian configuration of four large vegetal cells (macromeres A′–D′) and four small animal cells (micromeres a′–d′), with the animal quartet skewed clockwise by roughly 45° relative to the vegetal quartet (Fig. 1A, stage 4a; Fig. 1C). [In fact, the orientation of the B quadrant spiral cleavages are actually opposite those of the other three macromeres, i.e., levorotatory at the third and fifth cleavages and dextrorotatory at the fourth (Sandig and Dohle, 1988; Huang *et al.*, 1999); the significance of this deviation from typical spiral cleavage will be discussed later.] Subsequently, macromere D′ exhibits an extensively modified pattern of cleavage, giving rise to 5 bilateral pairs of medium-sized blastomeres called teloblasts and 16 additional small blastomeres (all of which we designate as micromeres) during the early phase of development (Fig. 1A, stages 4b–7). The teloblasts are embryonic stem cells; through repeated divisions, they each generate a coherent column (bandlet) of segmental founder cells called blast cells; four pairs of teloblasts (designated N, O/P, O/P, and Q) give rise to ectoderm, and one pair (designated M) gives rise to mesoderm (Fig. 1C). On each side of the embryo, the five bandlets come together in a parallel array, forming left and right germinal bands (not to be confused with the *Drosophila* germ band); the germinal bands are connected at their distal ends in the vicinity of the animal pole of the embryo (Fig. 1A and B, early stage 8). This is the prospective anterior end of the animal and contains the first blast cells produced from the teloblasts. The germinal bands and the animal territory between them are covered by a squamous epithelium derived from many of the micromeres.

Continuing divisions of the teloblasts add more blast cells to the proximal, more posterior ends of the germinal bands. As they do so, the germinal bands move over the surface of the embryo and gradually coalesce like a zipper from anterior to posterior, forming the germinal plate along the ventral midline (Fig. 1A and B, mid-stage 8 to stage 9). The movements of the germinal bands are accompanied by an expansion of the overlying squamous epithelium, which thus is undergoing epiboly. The basal surface of the squamous epithelium contacts a sparse network of mesodermally derived muscle fibers (Weisblat *et al.*, 1984). Together, these tissues make up the provisional integument, a temporary body covering for the embryo. The bulk of the embryo consists of the non-D quadrants and the yolky remnants of the teloblasts. Prior to the completion of epiboly, the germinal bands have disconnected from the columns of blast cells proximal to the teloblasts. Both mesodermal and ectodermal teloblasts produce more blast cells than are used to found the segmental tissues. It has previously been assumed that these supernumerary blast cells die (Shankland, 1984), but this now seems unlikely (Desjeux, 1995; Shankland, 1998; Desjeux and Price, 1999).

As cell division continues within the germinal plate, it spreads laterally and dorsally over the surface of the yolk (Fig. 2, mid-stage 9). Eventually its lateral edges meet along the dorsal midline, closing the tube that constitutes the main body of the leech (Fig. 2, stage 10). During this period, definitive epidermal and muscle cells replace the provisional integument and enclose the yolk. Also during this period, the "yolk mass," which marks the prospective midgut, changes from its initially spherical form, first to a pear-shaped mass and then gradually to the multilobed structure that is the midgut of the worm (Fig. 2, late stage 8 to stage 11). We use the ambiguous term "yolk mass" intentionally to defer the problem of defining it in terms of specific cells. When the proboscis has matured and the yolky contents of the midgut have been digested, the juvenile leech is ready for its first meal, in the case of *H. robusta*, a small freshwater snail.

The 11 stages of glossiphoniid leech embryogenesis referred to above were originally defined by Fernandez and Stent (1980) and later refined slightly (Stent *et al.*, 1992). Leech eggs are fertilized internally but arrest in first meiosis until after they are laid (zygote deposition), the beginning of stage 1; thus, we can also time developmental events in terms of hours after zygote deposition (hours AZD).

In standard accounts of leech embryogenesis, the A, B, and C quadrant macromeres are cast in passive and interchangeable roles, initially providing the substrate on which the morphogenetic cell movements of gastrulation are played out, and then later giving rise to or being enveloped by the gut and digested. But as shall be described in the following sections, we are now discovering that the A, B, and C quadrants play active and complex roles during cleavage, gastrulation, and gut formation. Moreover, in at least some of these processes, there is evidence of specific roles for each of the three quadrants.

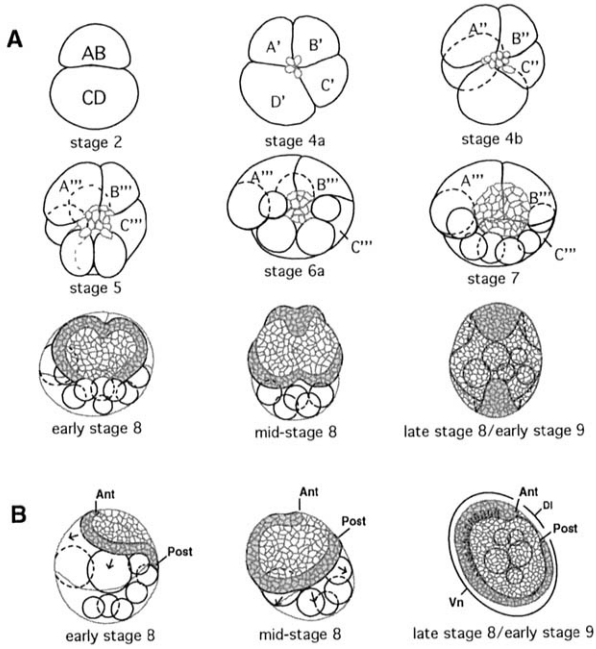

Fig. 1 Summary of leech development. (A) Relevant stages as seen from the animal pole (prospective dorsal views; posterior toward the bottom). The A, B, and C quadrant macromeres are labeled; micromeres (small contours) and the proteloblasts and teloblasts arising from the D quadrant are not. (B) Left equatorial views of stages 8 and 9 highlight the epibolic movements of the germinal bands and micromere-derived epithelium during gastrulation. By early stage 8, the germinal bands (grey) are joined at their anterior (Ant) ends and elongate through the addition of blast cells from the teloblasts at their posterior (Post) ends. During stage 8, they move ventrovegetally over the surface of the embryo (arrows) and gradually coalesce from anterior to posterior, forming the germinal plate (grey) along the ventral (Vn) midline. By stage 9, germinal plate formation is complete and C‴ has fused with A/B to form the syncytial yolk cell A/B/C; dorsal (Dl) territory is indicated. (C) Partial cell lineage diagram for *Helobdella*, emphasizing micromere production and the cell fusions entailed in formation of the gut precursor. The corresponding developmental stages and hours after zygote deposition are indicated on the time line at left; breaks in the time line denote changes in scale. The macromeres, proteloblast, and teloblasts are indicated in capital letters, as are the fusion products (A/B, A/B/C, and SYC). Blast cells are denoted by lowercase letters; micromeres are denoted by lowercase letters and primes (e.g., nopq′). Documented cell fusions are denoted by the merger of the various cell lines; dotted lines indicate the omission of bilaterally symmetric lineages (M_L and M_R; $NOPQ_L$ and $NOPQ_R$), the continuing production of blast cells from the teloblasts (M, N, O/P, O/P, and Q), and uncertainties in the timing of fusions of supernumerary blast cells and teloblasts other than the M and N.

II. Macromere Behavior during Cleavage

During stage 4, the A, B, and C blastomeres each undergo three highly unequal divisions, forming a macromere and three micromeres (Fig. 1C). The terminology used here to refer to the non-D quadrant cells is modified from the standard

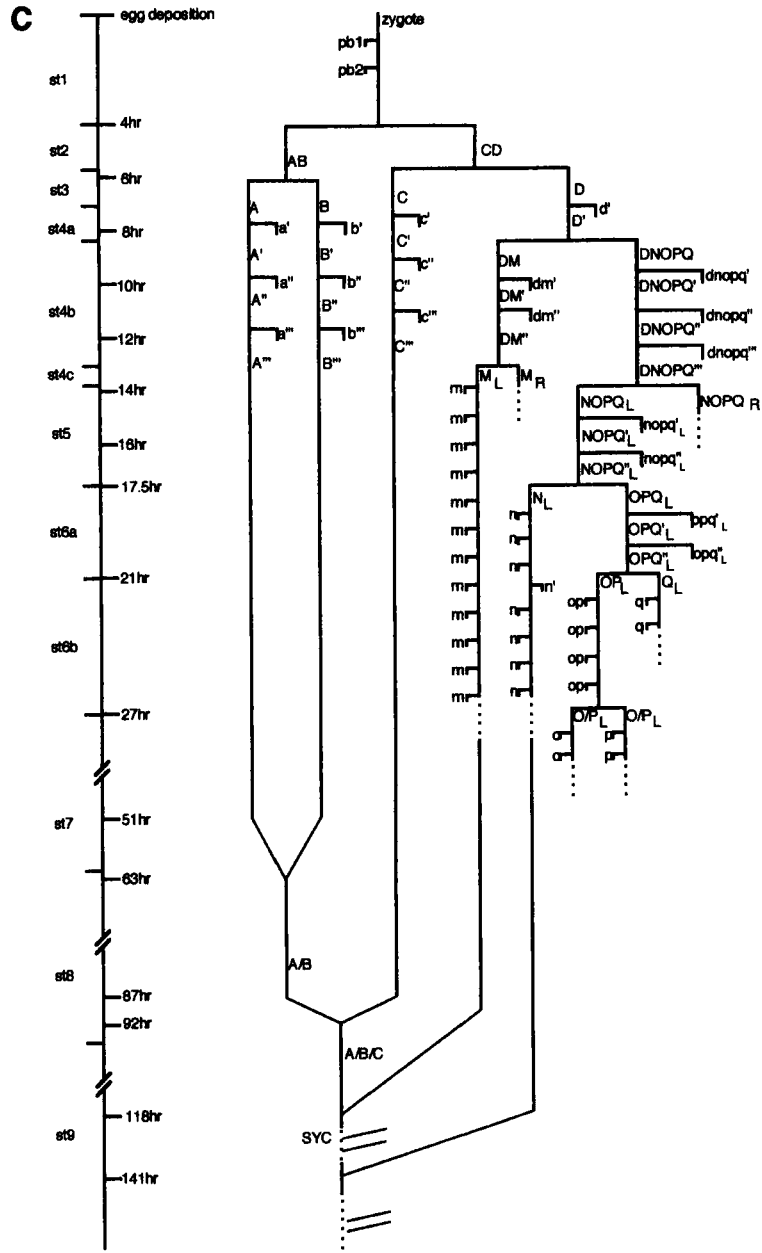

Fig. 1 (*continued*).

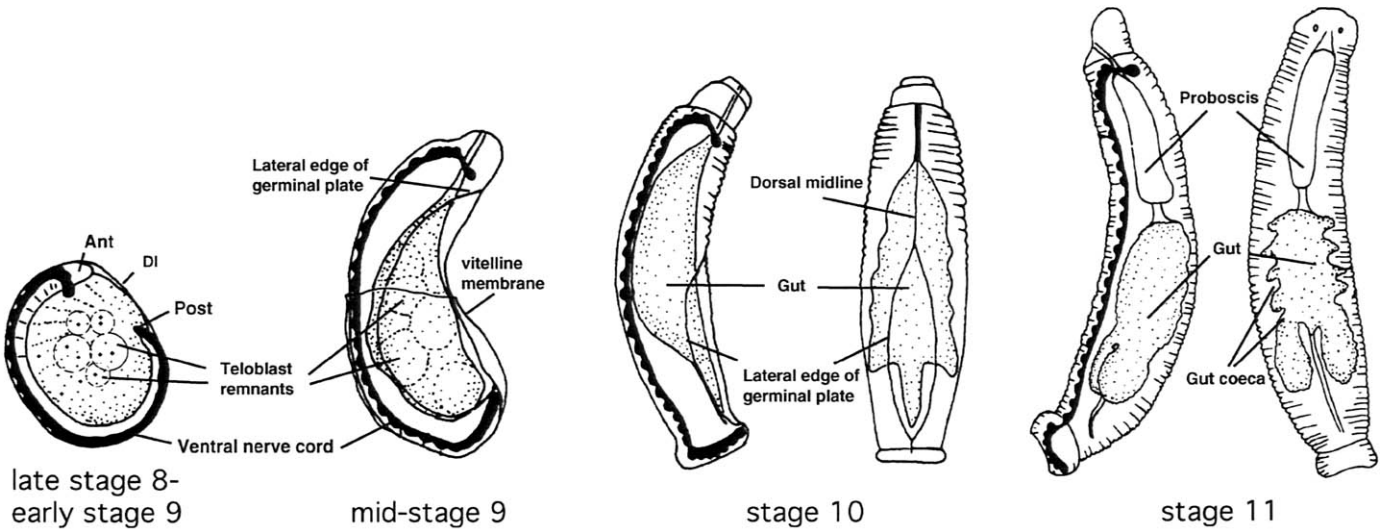

Fig. 2 Midgut morphogenesis in *Helobdella*. Lateral and dorsal views (stages 10 and 11) of later development. The yolk mass and developing midgut are denoted by stippling.

terminology applied to most annelid and other spiralian embryos (see Smith and Weisblat, 1994). At each highly unequal cleavage, the large and small daughter cells are designated by capital and lowercase versions of the parent cell, respectively and a prime (′) is added to each. Thus, the A quadrant macromere is designated A′, A″, and A‴ after third, fourth, and fifth cleavages, respectively (Fig. 1C). During these micromere-forming divisions, several differences between the A, B, and C quadrant cells emerge.

First, cell C is slightly older than cells A and B, because cell CD divides before cell AB at second cleavage and divides ahead of the A and B quadrants throughout the three rounds of micromere-forming divisions. The A and B lineages divide in synchrony, slightly after the C lineage. Another difference, first reported by Sandig and Dohle (1988), is that the B quadrant macromere divisions proceed with the opposite handedness of the A and C quadrants, in violation of canonical spiral cleavage. Thus, the A and B quadrant cells exhibit mirror symmetric divisions with respect to the AB cleavage plane formed at second cleavage.

Another potential difference between the C quadrant and the other two non-D quadrants emerges from investigations into the mechanisms of unequal cleavage in *Tubifex hattai.* Ishii and Shimizu (1995; Shimizu, 1996a) showed that the first mitotic spindle in this oligochaete annelid contains only one centrosome, as judged by γ-tubulin immunoreactivity, and is monastral by that criterion. This asymmetry causes the mitotic apparatus and cytokinetic furrow to be shifted to one side and thus leads to the unequal first cleavage; the cell inheriting the aster is the larger, CD cell, whereas cell AB lacks the aster. In CD, the centrosome replicates normally prior to the second cleavage, so that both the C and D daughters inherit one. [Thus, it seems likely that the unequal division of blastomere CD (at second cleavage) is established by a different mechanism than the unequal division of the zygote at first cleavage (Shimizu, 1996b); see also Symes and Weisblat (1992).] In contrast, the AB cell and its A and B progeny exhibit no γ-tubulin immunoreactivity and are classified as anastral in *Tubifex* by Ishii and Shimizu (1995; Shimizu, 1996a). Whether these features will apply to glossiphoniid leeches remains to be determined.

When the macromeres arise at third cleavage (Fig. 1A, stage 4A), they have relatively simple shapes, like the sections of an orange with only four sections. During stages 4–7, however, the A, B, and C quadrant macromeres undergo extensive and complex changes in shape and position, as cleavages in the D quadrant generate teloblasts (Fig. 3). We have been able to document these changes more accurately by injecting cells with a histochemically detectable enzyme, β-galactosidase. The intensely colored precipitate formed when this enzyme acts on a synthetic indolyl substrate remains insoluble even when the embryos are cleared with organic solvents such as benzyl benzoate/benzyl alcohol. This allows us to see the three-dimensional shapes of the cells by examining the fixed, stained, and cleared embryos at different stages, using transmitted light under the dissecting or compound microscope (Liu *et al.*, 1998) (Fig. 3).

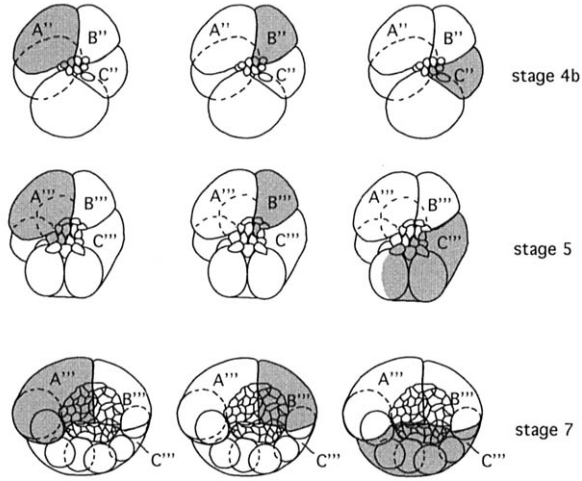

Fig. 3 Shape and positional changes of the A, B, and C quadrant cells during cleavage. From the time of their birth (stage 3) through stage 7, the A and B quadrant macromeres undergo little change in position or shape, while the C quadrant macromere spreads clockwise to engulf most of the teloblasts arising from the D quadrant.

As cleavages proceed within the D quadrant to form the 10 teloblasts and 16 micromeres during stages 4–6, the medium-sized teloblasts remain roughly spherical. The space around and between them in the embryo is taken up by the macromeres, chiefly macromere C‴, which consequently shifts clockwise relative to the D quadrant cells and assumes a highly complex shape (Fig. 3). During this time, macromere C‴ also seems to shift along the animal/vegetal axis, so as to occupy more territory at the vegetal pole of the embryo. Concurrently, the A‴ and B‴ macromeres come to lie in apposition across the midline of the embryo. A‴ and B‴ also shift to take up more territory at the animal pole beneath the micromere cap and withdraw from the vegetal pole.

The foregoing description of the movements of the A‴, B‴, and C‴ macromeres resolves the following paradox regarding the establishment of the anteroposterior (AP) axis and the bilateral symmetry of the early embryo. Since the time of Whitman (1878), four- and eight-cell leech embryos have been illustrated as in Fig. 4A/4B, with the AP axis bisecting the B and D quadrants. Representing the preceding, two-cell stage in this "D-centric" orientation, the first cleavage plane lies at an oblique angle with respect to the AP axis and the corresponding two-cell embryo lies as in Fig. 4A/4B. But it is aesthetically and perhaps even scientifically appealing to assume that the first cleavage is transverse to the AP axis (Fig. 4C). This "CD-centric" orientation leads to a four- and eight-cell embryo in which the B–D axis is oblique to the AP axis.

Is either view, the D-centric or CD-centric, a better representation of biological reality? In the CD-centric model (Fig. 4C), the A and B quadrant cells are sit-

uated in apposition at the embryonic midline from the time of their birth onward, in which case, the reverse handedness of the B quadrant cleavages casts the A and B quadrant cells and their progeny as mirror symmetric lineages with respect to the embryonic midline. In this reference system, the unequal second cleavage of cell CD forces a temporary displacement of the sister endodermal (C quadrant) and segmental (D quadrant) lineages. As C and D derivatives shift clockwise and counterclockwise, respectively, during later cleavages, this displacement is "corrected" with both C and D lineages straddling the midline.

The alternative, D-centric view (Fig. 4B) requires first that the AP axis is established with a fixed offset with respect to the first cleavage plane, because embryos can develop normally from zygotes in which the first cleavage plane was redirected by compression (Nelson and Weisblat, 1992). From this, it seems that the AP axis is determined by the first cleavage plane, rather than vice versa, or at least that the AP axis is not established irreversibly prior to first cleavage. Moreover, this reference system, with B initially straddling the midline, also entails a concerted clockwise shift of all three non-D quadrant macromeres, to bring A and B into bilaterally symmetric positions by stage 7. Thus, the D-centric view seems like a rather roundabout means for establishing embryonic axes in the leech, but Okham was almost certainly not an embryologist! [The question of how bilateral symmetry is established in spirally cleaving leech embryos is discussed further by Weisblat (1998).]

Another process in which the macromeres are involved during cleavage is the envelopment of the D quadrant derivatives by the non-D cells, primarily macromere C‴ (Fig. 3). It seems that this process must require substantial alteration of the cytoskeleton in the enveloping cell, perhaps triggered by the expression of new surface proteins on the nascent proteloblasts and teloblasts. We also observed that macromere C‴ spreads more than A‴ or B‴, enveloping most of the teloblasts and contacting all 10. By contrast, macromere A‴ contacts only three teloblasts by the beginning of stage 7, even though the A and C quadrant cells start out with equal access to the cleaving D quadrant cells. This apparent difference between the A‴ and C‴ cells is quantitative rather than qualitative, however. In embryos from which the C quadrant cell is cut away at stages 3–4a, teloblasts arise from the D quadrant and are enveloped by cells A‴ and B‴ (Isaksen *et al.*, 1999). These results should serve as a reminder that descriptions of cell-specific traits derived solely from normal development do not reveal whether the observed behaviors result from intrinsic differences between the cells or from extrinsic influences.

III. Syncytial Yolk Cell Formation

Three developmental pathways can be imagined by which yolky endodermal precursor cells could give rise to a definitive gut epithelium with the concomi-

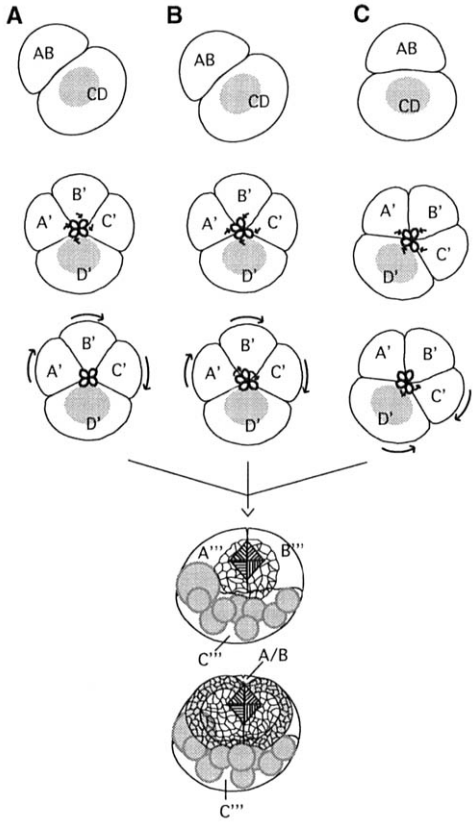

Fig. 4 Origins of bilateral symmetry in the *Helobdella* embryo. All embryos are depicted as viewed from the animal pole (with anterior up, according to each representation). Grey shading indicates teloplasm in the top three rows, and teloblasts and germinal bands in the bottom two rows (compare with Fig. 1). (A) The D-centric view with classical spiral third cleavage that is not seen in the leech. (B) The D-centric view indicating reversed B quadrant cleavage (Sandig and Dohle, 1988). (C) The AB-centric view with reversed B quadrant cleavage. In the D-centric representations, the first cleavage (top row) is oblique to the A–P axis, so that the D quadrant lies at the posterior pole. If the spiral third cleavage was completely dextrorotatory (A, second row), then the primary quartet micromeres (small circles) would arise with a′ and b′ as one left–right pair of cells, and d′ and c′ as another, with respect to the germinal bands, which indicate the bilateral plane of the adult (bottom row). This orientation is consistent with the distribution of their definitive progeny, as indicated schematically by the hatched triangles in the bottom two rows [a′ and b′ progeny, left and right diagonal hatching, respectively; d′ and c′, horizontal and vertical hatching, respectively; for more accurate representations on the positions of these cells, see Nardelli-Haefliger and Shankland (1993) and Smith and Weisblat (1994)]. But because the B quadrant cleaves with reverse handedness (B, second row), maintaining the D-centric representation requires positional shifts (arrows, third row) from the a′ and b′ micromeres as well as from the A, B, and C quadrant cells. In the AB-centric representation (C), the first cleavage is transverse to the A–P axis of the embryo, and the lateral displacements of the C and C quadrant cells are corrected when

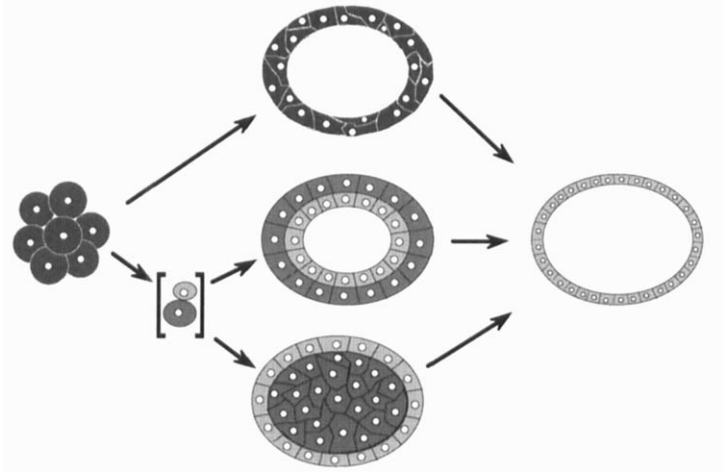

Fig. 5 Three pathways of midgut formation from yolky precursor cells. (For simplicity, surrounding mesodermal and ectodermal lineages are omitted from this schematic.) In one pathway, yolky precursor cells (left) cleave directly to form a hollow tube of similar, yolk-rich cells around the prospective gut lumen (center top); the yolk within them is gradually digested, giving rise to the midgut epithelium (right). Alternative pathways entail the division of the yolky precursor cells into distinct epithelial and yolk lineages (bracketed cells, light grey and dark grey, respectively). These lineages could then develop with the yolk either on the outside (center middle) or on the inside (center bottom) of the prospective gut epithelium.

tant absorption of the yolk (Fig. 5). In one pathway, the initially solid mass of yolk cells gives rise to the epithelium directly, cleaving to form a cellular tube that defines the lumen of the gut; in this path, the yolk is maintained intracellularly by the nascent gut epithelial cells (Fig. 5, top). In the other pathways, the endodermal precursors give rise at some point to separate epithelial and yolk cell sublineages; within this general scheme, the yolk cells could be either inside (Fig. 5, bottom) or outside (Fig. 5, middle) of the prospective gut, as defined by the epithelial cells. As reviewed by Anderson (1973), the midgut epithelium arises by variations of all of these routes in different annelid species. For example, in *Tubifex* (an oligochaete annelid), the definitive gut arises more or less directly

---

C‴ envelopes the nascent teloblasts during late cleavage (C, third row). In this representation, micromeres a′ and b′ arise as a left–right pair and only cells c′ and d′ (or their progeny) must shift to reach their definitive positions (C, third row). By the time cleavage is complete (fourth row), most of the teloblasts are completely enveloped by macromere C‴, and macromeres A‴ and B‴ occupy portions near the animal pole of the embryo that were originally occupied by macromere C‴. This symmetry is maintained through germinal band formation (fifth row), by which point macromeres A‴ and B‴ have fused, forming cell A/B (from *Hydrobiologia*, 1999; Cellular origins of bilateral symmetry in glossiphoniid leech embryos; D. A. Weisblat; Fig. 3, © 1999 Kluwer Academic Publishing; reproduced with kind permission from Kluwer Academic Publishers).

from the yolk cells, so the yolk remains inside of the prospective gut epithelial cells and the gut lumen arises as a hollowing out of this mass of dividing yolk cells. By contrast, in *Rhynchelmis* (oligochaete) and *Capitella* (a polychaete annelid), the definitive gut arises as a hollow epithelial ball surrounded by the yolk cells, so the yolk lies outside the lumen of the nascent gut. Glossiphoniid leeches are an example within the annelids of the third pathway, in which the epithelium arises outside the yolk cells and surrounding them.

Many of these routes to forming the gut epithelium involve syncytial yolk cell intermediates. Syncytial cells can arise by cell fusion, as in the formation of mammalian striated muscle by myoblast fusion, and/or cytokinesis without karyokinesis, as in the *Drosophila* blastoderm. In *Drosophila,* the wave of cellularization that occurs after the thirteenth round of nuclear proliferation forms precursors for all the gut tissues simultaneously with the mesodermal and ectodermal precursors. These cells arise at the surface of the embryo and are internalized later during gastrulation (Fig. 6). In glossiphoniid leeches, by contrast, holoblastic cell divisions separate mesodermal, ectodermal, and endodermal pre-

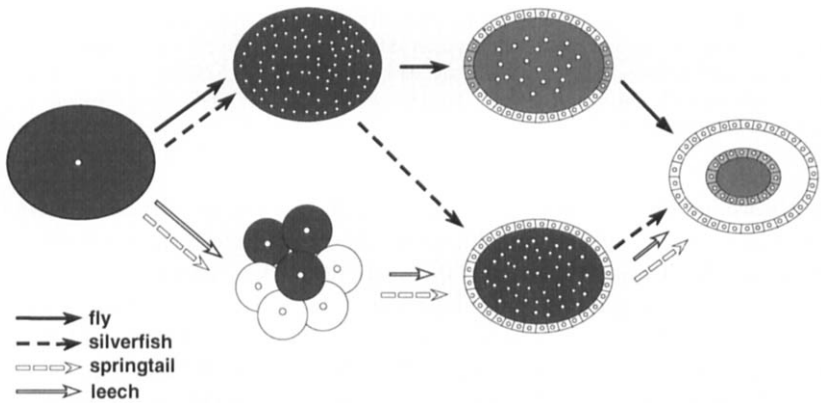

Fig. 6 Syncytial yolk cells in the leech, the fly, and wingless insects. In *Drosophila*, the nucleus of the zygote (far left) proliferates directly to form a yolky syncytial blastoderm (top left). Cellularization of the syncytial blastoderm (top right) puts precursors of the midgut epithelium (light grey) at the surface of the embryo. These midgut precursor cells move inside and surround the residual yolk (far right) as a result of cell movements during gastrulation. In this simplified version of leech development, complete cleavages (lower left) lead to early segregation of mesodermal and ectodermal lineages (white) from midgut precursors (dark grey). A syncytial yolk cell (lower right; dark grey) arises later as the result of cell–cell fusions among the midgut precursors (plus spent teloblasts and supernumerary blast cells from the mesodermal and ectodermal lineages). Cellularization of the syncytial yolk cell results in the formation of the definitive midgut epithelium surrounding the residual yolk. Wingless insects exhibit hybrid pathways of gut formation. In Thysanura (silverfish and bristletails), the zygote forms a syncytial blastoderm, but in the initial cellularization, precursors of the midgut epithelium remain in the syncytial yolk cell, resulting in an intermediate stage that is similar to the leech embryo. Collembola (springtails) resemble leeches even more closely, in that initial cleavages are complete and a syncytial yolk cell forms by cell fusion interior to the blastoderm.

cursors during cleavage and cell fusion is part of the later process by which endodermal precursors give rise to the definitive midgut epithelium (Fig. 6). Endodermal precursor cells (A‴, B‴, and C‴) fuse to form a syncytial yolk cell (Liu *et al.*, 1998), within which nuclei continue to proliferate. Eventually, some of the syncytial nuclei migrate to the periphery and cellularize to form the midgut epithelium (Nardelli-Haefliger and Shankland, 1993). By this means, the definitive gut forms around the yolk cells, which therefore lie within the lumen of the nascent gut, as stated above.

A similar process of midgut formation by cellularization of yolk nuclei that were never part of the blastoderm has been described for wingless insects such as the Thysanura (bristletails and silverfish). We might consider these insects as undergoing two waves of cellularization of syncytial yolk nuclei. The first wave forms the cellular precursors of the segmental ectoderm and mesoderm, plus the foregut and hindgut. The second wave forms the cellular precursors of the midgut epithelium (Fig. 6). Another group of wingless insects, the Collembola (springtails), are even more similar to leech, in that they undergo holoblastic cleavages initially and then later form a syncytial yolk cell by the fusion of precursor cells within the blastoderm (Fig. 6). These parallels between the process of midgut formation in annelids and basal arthropods raise the possibility that the process of gut formation from a syncytial yolk cell is ancestral to both groups and that the syncytial blastoderm of the more derived insects has evolved from the syncytial yolk cell of the ancestor. This area seems ripe for further analysis and comparisons, applying the more sophisticated lineage tracing techniques and molecular markers now available.

Whitman (1878) concluded that the epithelial lining of the gut in glossiphoniid leech arises from multinucleate A‴, B‴, and C‴ macromeres, but he seemed unaware that these cells fuse with one another, stating, "I have found that these blastomeres preserve their individuality during the entire period of invagination and neurulation. . . ." A clear appreciation of the fusion process was provided by Bychowsky (1921), however, who reported a gradual loss of visible outlines for the yolk cells, beginning at the anterior end of the prospective midgut. Judging from his drawings, he was referring to embryos at early stage 9, by which time the germinal plate has completely formed.

In our laboratory, we have used a more sensitive assay to observe cell fusion, namely, the visualization of readily detectable macromolecules that diffuse between cells that have fused. For this purpose, we have employed β-galactosidase and fluorescently labeled dextran molecules as microinjected lineage tracers, with equivalent results (Liu *et al.*, 1998). We find that the three macromeres fuse in a stepwise manner to initiate formation of the syncytial yolk cell. The first step is the fusion of macromeres A‴ and B‴ to form a cell we designate as A/B (Fig. 1C). When we injected β-galactosidase into either the A or the B quadrant cell during stages 4 to 5 and then stained at progressively later times, we detected diffusion of the enzyme from one cell into the other (as determined by the distrib-

ution of the histochemical reaction product) as easily as midstage 7; thus, A‴–B‴ fusion occurs during the time interval corresponding to 51–63 hr of AZD. In *Helobdella*, this is approximately 65 hr before the stage at which Bychowsky (1921) inferred fusion by the loss of visible cell outlines within the yolk mass. At about the end of stage 7 (approximately 12 hr later), macromeres A‴ and B‴ had fused in virtually all embryos in a batch. Macromere C‴ fuses with A/B at the end of stage 8 (87–92 hr AZD), approximately 25 hr after the A‴–B‴ fusion, yielding a cell we designate as A/B/C (Fig. 1C).

Despite the fact that fusion has occurred, the cleavage furrow between what were separate macromeres remains distinct for about 24 hr after fusion is first evident by the diffusion assay. We observe, as did Bychowsky (1921), that the disappearance of the furrows proceeds from anterior to posterior. Electron microscopic analysis of the fusion process confirmed the perdurance of the apical junction structures between the nominal A‴ and B‴ cells well after fusion had occurred (Liu *et al.*, 1998).

Specifically, we analyzed the membranes of A‴ and B‴ where they contacted one another and where each contacted C‴, in embryos fixed at least 14 hr after fusion had occurred, as judged by observing the diffusion of fluorescent lineage tracers from one cell to the other. The first obvious breakdown of membranes between the fusing A‴ and B‴ cells consisted of gaps up to 3 μm wide. No such gaps were observed in embryos fixed prior to fusion. These gaps extend through multiple serial sections and are bounded by islands of flattened double membrane, presumably formed by the joining of the nominal A‴ and B‴ membranes. Even in the embryos that had initiated fusion many hours before, the gaps were seen only at the animal end of the embryo, near the surface of the embryo where the macromeres are also in contact with blast cells and micromeres. The tight junctions and other structures associated with the apical junctions of the macromeres still appear normal at this point, which explains the perdurance of the cleavage furrows relative to the actual cell fusion events. The observation that the membrane breakdown initiates at the animal end of the embryo is consistent with Bychowsky's (1921) report that loss of visible yolk cell boundaries occurs progressively from anterior to posterior within the yolk mass. A somewhat similar description of cell–cell fusion in the nematode hypodermis has been published (Mohler *et al.*, 1998). The appearance of the fusion pores specifically at the animal end of the embryo suggests the possibility that macromere fusion may be regulated or induced by signals emanating from the blast cells and/or micromeres. This possibility is explored in the next section.

Schmidt (1939) proposed that the M teloblasts of glassiphoniid leech embryos fused with the macromeres on the basis of light microscopic examination of sectioned embryos of somewhat indeterminate age. We used the diffusion assay to confirm and extend Schmidt's findings. M or N teloblasts were injected with a fluorescent lineage tracer during stage 6, and the resultant embryos were fixed and cleared at various times, beginning at the end of stage 8. We designate the

cell resulting from the fusion of teloblasts with A/B/C as the syncytial yolk cell (SYC; Fig. 1C). We find that M teloblast fusion occurs during the period 89–118 hr AZD. The N teloblast fusion occurs over an even later time period, during the interval of 118–141 hr AZD. This result is consistent with the fact that the M teloblasts finish producing their full complement of segmental founder cells 35 hr earlier than the N teloblasts (Zackson, 1984; Weisblat and Shankland, 1985; Lans *et al.*, 1993).

Near the end of blast cell production, each teloblast generates "supernumerary" blast cells that are not incorporated into the germinal bands or germinal plate. It was originally supposed that these cells die (Shankland, 1984), but recent experiments suggest that, like the teloblasts, these cells fuse with the endodermal lineage instead of dying (Desjeux, 1995; Shankland, 1998; Desjeux and Price, 1999). This would mean that the teloblasts and their supernumerary blast cells contribute to the gut epithelium, an endodermal tissue, as well as to segmental mesoderm and ectoderm, an observation that further muddies the significance of the classical germ layer designations [as do the precise lineage analyses in animals such as the nematode *Caenorhabditis elegans* (Sulston *et al.*, 1983)]. Thus, the syncytial yolk cell receives contributions of nuclei (and cytoplasm) from three embryonic lineages—the macromeres, the teloblasts, and the supernumerary blast cells. Whether these different components contribute equally to the definitive gut epithelium and the remaining yolk nuclei remains to be determined.

IV. Regulation of Macromere Fusion

The B quadrant cell and its descendant B′–B‴ macromeres are in constant contact with their counterparts in the A and C quadrants from stage 3 onward (Figs. 1 and 3), yet macromere B‴ fuses selectively with A‴ only after 45–57 hr, with C‴ only after 81–86 hr, and with the teloblasts yet later (Fig. 1C). The regulation of the timing and specificity of the fusion process presents a fascinating cell biological puzzle that we have only just started to investigate (Isaksen, 1997; Isaksen *et al.*, 1999).

The first evidence regarding the source of the regulation of the fusion process came from embryos that were removed from the fertilization membrane, so as to be amenable to microsurgical cell ablation after injecting the A and B cells with fluorescent lineage tracer to monitor fusion. When cell C is removed from such embryos, the remaining quadrants undergo apparently normal subsequent divisions and macromeres A‴ and B‴ fuse as in controls. Moreover, in such embryos, the nascent teloblasts became embedded by the remaining macromeres; thus, the process of teloblast envelopment seems unlikely to be the explanation for why C‴ fusion is delayed relative to A‴–B‴ fusion in intact embryos.

In contrast to the foregoing results, when macromere D′ is removed from the

embryos, macromeres A‴ and B‴ fail to fuse. This result suggests that signals from the D quadrant are required for A‴–B‴ fusion to proceed normally. But to control for the possibility that the trauma of removing macromere D′ blocked macromere fusion artifactually, we sought to interfere with the biochemical activity of selected cells *in situ* by microinjecting them with the ricin A chain, a potent inhibitor of eukaryotic translation (Endo and Tsurugi, 1988), or with RNase A. Cells injected with either of these reagents round up and undergo at most one further division, but do not lyse (Nelson and Weisblat, 1992; Isaksen *et al.*, 1999); we therefore refer to the injected cells as being "biochemically arrested" (Smith *et al.*, 1996).

Consistent with the cell ablation results, biochemical arrest of the C quadrant cell has no effect on A‴–B‴ fusion, whereas arresting the D cell blocks A‴–B‴ fusion (Fig. 7). The relative simplicity of the biochemical arrest technique also allows us to extend these experiments to later stages of development, for which the microsurgical approach is not feasible. Thus, in subsequent experiments, we arrested progeny of macromere D′ at progressively later times in development. If we wait until macromere D′ has cleaved and then arrest the two daughter cells DM and DNOPQ at stage 4b, fusion is still blocked in almost all of the embryos (Fig. 7). However, by delaying the arrest by a few hours and then arresting DM″ and DNOPQ‴ by ricin injection at stage 4c, then most embryos fuse (Fig. 7).

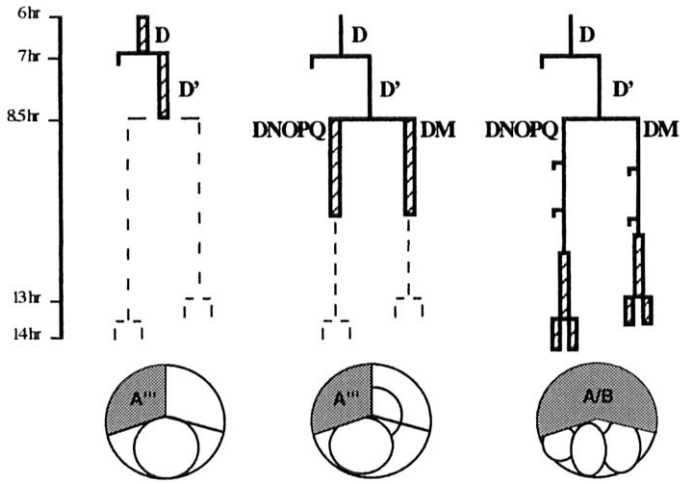

Fig. 7 Biochemical arrest of D lineage blastomeres blocks a‴–B‴ fusion, with an early critical period. The D quadrant was arrested by microinjection of ricin A chain into blastomere D, macromere D′, or the descendant proteloblasts (DM and DNOPQ) at times indicated by the hatched bars; the time line at left is as in Fig. 1C. Results (assessed at about 75 hr after zygote deposition) are indicated schematically below each lineage diagram. Note that the cells injected with ricin no longer divide. Biochemical arrest of D, D′, or early DM and DNOPQ lineages block a‴–B‴ fusion, whereas later injections of DNOPQ″ and DM″ do not. Other experiments are described in the text (from Weisblat *et al.*, 1998).

Between stages 4b and 4c, the D quadrant cells have given rise to five additional micromeres (dm′, dm″, dnopq′, dnopq″, and dnopq‴), which were not injected with ricin in the experiments described above. Does this mean that some or all of these micromeres are required for the fusion signal? Apparently not, because fusion is observed in a substantial fraction (20–30%) of embryos in which cell DM and all three dnopq micromeres were arrested by ricin injection, so that cell DNOPQ‴ is allowed to continue cleaving. Fusion is also seen in most embryos if either DM or DNOPQ is allowed to continue cleaving. We conclude that the capacity to induce fusion is distributed among the D quadrant progeny and that A‴–B‴ fusion is largely immune to the effects of D quadrant arrest by the end of stage 4. There are two main interpretations for these observations. One is that the putative D-derived signal has already been sent by stage 5. The other is that the signal is still in the D quadrant derivatives, but that its transmission is immune to the ricin-induced biochemical arrest after the end of stage 4. For example, assuming that the injected ricin A chain acts by inhibiting protein synthesis, one possibility is that the required D lineage signal involves a protein that is synthesized during stage 4, but becomes active only in response to a posttranslational modification much later in development. In any case, it is striking that the critical period of ricin sensitivity ends at least 40 hr before fusion actually occurs.

In another series of experiments, we examined the effects on A‴–B‴ fusion of arresting A and B quadrant cells with ricin or RNase injections. We found a time course of sensitivity similar to that obtained for D quadrant arrest. That is, arresting either cell prior to stage 4b with ricin injection effectively blocked fusion, whereas both cells were immune to the effects of ricin injection after stage 4c. Within the transition period, we found (much to our surprise) that macromeres of the A lineage become resistant to the effects of ricin injection several hours prior to B lineage macromeres, despite the fact that the lineages arise via synchronous divisions from A and B blastomeres that arise as sisters by an equal division at second cleavage, and had been presumed by us to be identical. We note that the A quadrant cell has a significantly greater area of cell surface contact with cell D and its derivatives than does cell B. It is also noteworthy that here, too, the fusion process becomes immune to the effects of ricin injection many hours prior to the actual fusion. Moreover, because arrest of either A or B can block fusion, we conclude that both A‴ and B‴ play an active role in fusion.

V. Epiboly

The most dramatic and visible aspect of gastrulation in glossiphoniid leech embryos is the ventrovegetal movements of the germinal bands that lead to germinal plate formation during stage 8. The movements of the germinal bands are accompanied by epiboly of the micromere-derived epithelium, which, together

with a network of underlying muscle fibers of mesodermal origin, comprise the provisional integument of the embryo. Little is known about how epibolic cell movements come about in any embryo, but superficially, the cell movements in leech resemble the epiboly seen in teleost fish, where the process is probably better studied than in any other organism (Trinkaus, 1984; Keller and Trinkaus, 1987; Solnica-Krezel and Driever, 1994). To understand the possible role(s) that macromeres might play in this process, we first need to review what is known about the contributions of other cells.

To distinguish the contributions of the micromere-derived epithelium and germinal bands in the epibolic movements of gastrulation, ricin-mediated biochemical arrest was used to ask whether the epithelium is able to undergo its normal gastrulation movements in the absence of the germinal bands and vice versa (Smith *et al.*, 1996). The results of these experiments have led us to appreciate the possibility that the macromeres may well be actively involved in the cell movements, rather than just providing a passive substrate for the movements of the overlying cells.

Embryos with a complete epithelium but lacking germinal bands can be generated by injecting teloblasts and proteloblasts with ricin A chain after all the various micromeres have been produced. The converse experiment, arresting the epithelial precursors while leaving the teloblasts intact, is impossible on several grounds, not the least of which is that it would require the successful injection of 17 small cells in each embryo (Smith and Weisblat, 1994). But it is possible to reduce the population of epithelial cells by roughly one-third by deleting just five micromeres, because there is no regulative replacement of the missing epithelial cells, at least in early development (Smith *et al.*, 1996).

A. Embryos without Germinal Bands

In embryos without germinal bands, the epithelium still undergoes epiboly but its expansion is abnormal in certain respects. First, the epithelial expansion is delayed, in that the vegetal translation of the leading edge is delayed with respect to control embryos (Fig. 8A). Though the expansion is delayed, the epithelial surface area seems to increase as in controls, with the result that the epithelium buckles and folds over itself. It seems that the epithelium is committed to an early expansion of its surface area (presumably by flattening of the epithelial cells) independent of any movement by its leading edge. Second, in embryos without germinal bands, the leading edge of the epithelium is typically very irregular. Contours of individual cells protrude from the margin, as in a mosaic of irregularly shaped tiles. In control embryos (Fig. 8B), the leading edge is quite continuous, as if parts of the tiles at the edge had been cut off to form a smooth border. Perhaps a closer analogy would be to imagine a mosaic of elastic tiles. In its relaxed state the cells at the edge would protrude, but placing the edge under tension would tend to straighten it, just as stretching a piece of wrinkled clothing

flattens it. Thus, both of these abnormalities of the micromere-derived epithelium in embryos without germinal bands can be explained by assuming that, in normal development, the epithelium is placed under tension in early epiboly. The forces generating this tension must arise from the germinal bands and/or the macromeres, because those are the only other cells in the embryo at this point.

B. Embryos with Reduced Epithelium

In embryos with reduced numbers of micromere-derived epithelial cells, the germinal plate forms more or less normally, but by late epiboly, the apical surfaces of individual epithelial cells are greatly expanded relative to those in controls

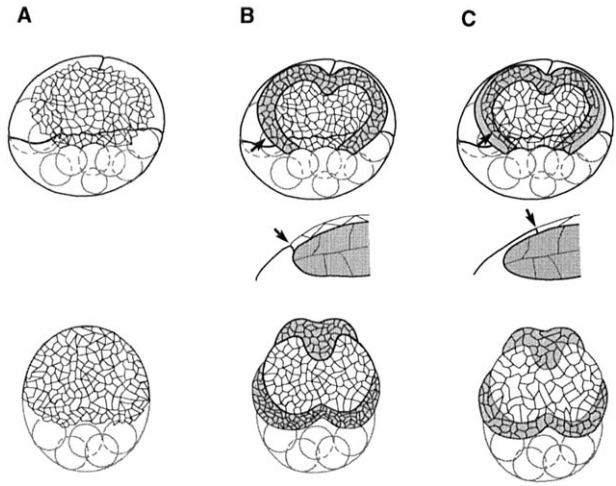

Fig. 8 Experimental perturbations of epiboly (Smith *et al.*, 1996). Schematic representations of embryos at early stage 8 (top row) and midstage 8 (bottom row), as viewed from the dorsal–posterior side of the animal pole. (A) Embryos in which teloblasts (medium circles) have been arrested by microinjection with ricin A chain lack germinal bands. In such embryos, the micromeres (small contours) still proliferate and spread from animal to vegetal territory, but somewhat more slowly than in normal embryos; moreover, the leading edge of the micromere-derived epithelium is often irregular. (B and C) When teloblasts are allowed to divide normally, germinal bands (grey) originate in animal territory and then move vegetally over the surface of the embryo. (B) In normal embryos, a cross-section through the germinal bands (middle drawing; taken at the position indicated by the arrow in the upper drawing) shows that the boundary between the macromere and the leading edge of the micromere-derived epithelium (arrow) is roughly in register with the leading edge of the germinal band. (C) By contrast, in embryos with reduced numbers of micromere-derived epithelial cells, the leading edge of the germinal band initially advances ahead of the micromere-derived epithelium (upper drawing); the corresponding cross-sectional view (middle drawing) reveals that the macromere is deformed to remain in contact with the micromere derivatives. By midstage 8, the micromere-derived epithelial cells have expanded dramatically relative to those in control embryos and their leading edges are back in register with the germinal bands.

(Fig. 8C). The most interesting deviation from controls is seen in early epiboly, however. Whereas the leading edges of the epithelium and germinal bands normally remain in close proximity throughout epiboly (Fig. 8B), in embryos with reduced numbers of epithelial cells, the germinal bands are well out in front of the leading edge of the epithelium throughout much of their length (Fig. 8C). The germinal bands are not exposed to the perivitelline space, however, nor has the leading edge of the epithelium detached from the underlying yolk cell. Instead, a broad, thin portion of the macromere extends over the germinal bands in such embryos, thereby retaining the continuity of the connection between the macromere and the epithelial margin (Fig. 8; cross-sectional views). It seems that something causes the germinal bands to translocate vegetally and the epithelium normally expands concomitantly with this movement. But when the epithelium contains fewer cells, its ability to expand is reduced and the resulting imbalance of forces is resolved by deforming the macromere instead.

What is the source of the force? The fact that the germinal band moves out ahead of the epithelial margin in the experimental embryos argues against the possibility that the germinal bands are being pushed or pulled by the epithelium. Another possibility is that the force for the early movements of the germinal bands and epithelial expansion could originate in the germinal bands, either from active movements of individual blast cells or through bending forces resulting from the increasing length of the germinal bands (as teloblasts keep adding new blast cells to their posterior ends).

In either case, the proposed force originating from the germinal bands is not the only one acting during epiboly. In late epiboly, the epithelial margin is in advance of the germinal bands, even in the embryos that have reduced numbers of epithelial cells and that are severely expanded relative to the situation in normal embryos. At that stage, after the epithelial margin has passed the equator of the embryo, we can imagine that contractile forces around the epithelial perimeter could act like a purse string, drawing it toward the vegetal pole.

The remaining candidate for contributing locomotive forces, both in early and late epiboly, is the macromeres. In fish, it appears that cortical contraction of the yolk cell cortical cytoplasm provides a force that essentially tows the leading edge of the blastoderm epithelium vegetally during epiboly (Trinkaus, 1984). Perhaps a similar process is at work within the yolk cell of the leech. Of course, these possibilities for the sources of the forces driving epiboly are not mutually exclusive. Indeed, the fact that the epithelial margin trails the edge of the germinal bands during early epiboly and leads it during late epiboly makes it seem likely that different combinations of forces are acting during different phases of epiboly.

C. A Possible Role for the Macromeres in Epiboly

The fact that the macromeres are so deformed in the embryos with reduced numbers of micromere-derived epithelial cells indicates that there is a strong me-

chanical connection between the yolk cell and the epithelial margin. Examining this boundary by electron microscopy in normal embryos, we find the typical structures associated with an apical epithelial junction, such as tight junctions and anchoring junctions (Isaksen, 1997). Presumably, the cytoskeletons in adjoining cells are linked via transmembrane proteins such as cadherins. Similar structures are seen at the surface of the embryo where the macromeres meet one another.

Thus, we may also view the macromeres as giant epithelial cells, whose apical surfaces are lost during epiboly. If, as it seems, the leading edges of the micromere-derived epithelium are firmly tethered to the macromeres, then apical constriction of the macromeres could provide the initial force required to expand the micromere-derived portion of the epithelium toward the vegetal pole (Fig. 9). Consistent with this notion, we find that epiboly is not blocked by treating the embryos with nocodazole, but is blocked by treating the embryos with 1,4-butanedionemonoxime (BDM) (E. Cheng, personal communication). BDM inhibits muscle and nonmuscle myosin ATPase activity (Backx *et al.*, 1994; Cramer and Mitchison, 1995). Because of its low molecular weight and good solubility, BDM, like nocodazole, diffuses throughout the embryo; therefore, these experiments do not reveal whether these pharmacological agents block epiboly by effects on macromeres, or on other cells.

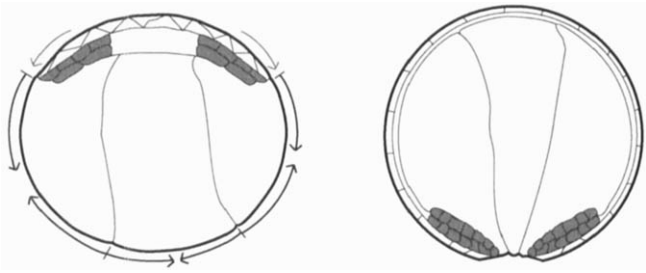

Fig. 9 A model of epiboly driven by apical constrictions of yolk cells. Schematic cross-sections through *Helobdella* embryos at stages corresponding to early and late epiboly. The animal pole is up. At early stage 8 (left) germinal bands (grey) occupy animal territory, covered by micromere-derived epithelial cells (white triangular contours) and lying atop the yolky macromeres (large irregular contours). In this model, we view the entire surface of the embryo, including both the micromere derivatives and the macromeres, as the apical surface of an epithelium (thick line), with the cortical cytoskeleton linked from cell to cell via the specializations at the apical junctions. The apposing faces of these cells (thinner lines) comprise the basolateral surfaces of the epithelial cells. During epiboly the germinal bands move across the surface of the embryo from animal to vegetal territory, and their movement is accompanied by the expansion of the micromere-derived epithelium (light arrows). Apical constrictions (heavy arrows) within the three macromeres could provide the force needed to tow the germinal bands and the leading edge of the micromere derivatives vegetally. The contribution from this source might be especially important during early epiboly, when the germinal bands are still on the animal side of the embryo and purse string forces at the leading edge of the micromere derivatives would act against epiboly.

In hopes of blocking epiboly using a cell-specific technique, we examined the effects on epiboly of "biochemically arresting" individual macromeres in the A, B, or C quadrants by intracellular microinjection of ricin A chain, which is confined to the injected cell (Smith, 1994; Liu *et al.*, 1998). As described above, the ricin-injected macromere rounds up, and consequently becomes partially enveloped by the other macromeres, but does not lyse. The remaining cells in the embryo seem unaffected; for example, the rate at which teloblasts produce blast cells is not affected when ricin is injected into any of the macromeres.

Of course, the biochemical actions of ricin and BDM are not at all the same, but in undertaking these experiments, it was hoped that ricin would block all biochemical processes in the affected cell through its general inhibition of protein synthesis. In fact, when either the A or B quadrant cells were injected, the coalescence of the germinal bands proceeded slightly slower than in uninjected controls, as judged by the numbers of left and right mesodermal hemisomites that had coalesced within a set time, but did not cease. By contrast, when the C quadrant macromere was poisoned, ~30% of the embryos exhibited a substantial increase in germinal band coalescence relative to controls!

These results are subject to a variety of interpretations. Perhaps the A and B cells play only a passive role in the epibolic cell movements of gastrulation. Or it may be that when either the A‴ or the B‴ macromere is poisoned the other one can take its place. Or perhaps the role of the A‴ and B‴ macromeres in epiboly is not appreciably affected by ricin poisoning (presumably an inhibition of protein synthesis). We suspect that the acceleration of germinal plate formation after biochemical arrest of the C‴ macromere results secondarily as the teloblast and bandlets of blast cells are forced to the surface of the embryo by the rounding up of the C‴ macromere in which they are normally embedded. Clearly, further experiments, using more specific and selective reagents, are needed to pursue these questions.

VI. Conclusions

In the adult forms of leeches and other annelid worms, segmental mesoderm and ectoderm comprise most of the animal. Thus, it is not surprising that it is the genesis of these tissues that has garnered the most attention from developmental biologists studying leeches. This tendency has been reinforced in recent years by the tantalizing prospect of comparing the sequential, holoblastic segmentation process in leeches with the simultaneous, syncytial segmentation process in flies (e.g., Weisblat *et al.*, 1994). But the purpose of this article has been to highlight what is known, and how much remains to be learned, about the contributions of the A, B, and C quadrant macromeres to the development of the leech embryo. These cells exhibit a variety of complex and fascinating behaviors that merit that attention of cell, developmental, and evolutionary biologists.

A. Cleavage

It is curious that the B quadrant macromere cleaves with the opposite handedness of the A and C (and D) quadrants during three rounds of micromere production (Sandig and Dohle, 1988). Given that this feature of glossiphoniid leech development escaped notice for over a century, we are led to wonder whether the "classical" unidirectional spiral cleavage (in which all four quadrants cleave in the same direction, with dextral and sinistral cleavages alternating) is as general as it appears. There are clear and detailed descriptions of true classical spiral third cleavages even within the annelids, e.g., the polychaete (Wilson, 1892). Thus, this reversal of the handedness of the B quadrant cleavages with respect to the A, C, and D quadrants may be a relatively new feature, perhaps unique to the glossiphoniid leeches. In any case, the pattern of B quadrant cleavage in leech reinforces the notion that A and B serve as contralateral homologs in these embryos and therefore that the first cleavage plane is oriented transverse to the prospective A–P axis.

We have also noted here the dramatic deformation of the non-D quadrant macromeres to accommodate the cleavages occurring in the D quadrant and to envelop the teleoblasts and their precursors. In normal embryos this behavior is normally most pronounced in the C quadrant macromere, which might be taken as evidence of cell-specific properties. But we note that in embryos from which the C quadrant macromere has been deleted, teloblasts are enveloped by processes of the remaining macromeres.

B. Syncytial Yolk Cell Formation

That the formation of the leech midgut epithelium proceeds by cellularization of a multinucleate syncytium suggests a possible homology at the cellular level between the embryogenesis of glossiphoniid leeches and *Drosophila.* This possibility is strengthened by comparison with previous descriptions of gut formation in other arthropods, as reviewed by Anderson (1973). Wingless insects, in which the developmental processes are more likely to resemble those in the ancestral form, also develop via a syncytial blastoderm. But in these insects, it seems that syncytial yolk cell nuclei migrate to the periphery of the yolk cell and become cellularized at two separate times in development. The first wave gives rise to a blastoderm containing mesodermal and ectodermal precursors, but the midgut precursors arise only from the second wave of cellularization. In contrast, in winged insects such as *Drosophila*, the blastoderm arising from the syncytial yolk nuclei already contains midgut precursor cells. The midgut epithelium is formed by epithelia of blastodermal origin that spread over the yolk from the anterior and posterior ends of the embryo.

Combining these observations with the data from leech, it is tempting to spec-

ulate that formation of the midgut epithelium by cellularization of a multinucleate syncytium was a feature of the common ancestor of annelids and arthropods, and may have arisen early in the protostome lineage, while the derivation of mesoderm and ectoderm from the syncytium arose more recently, within the arthropod lineage. The mollusks are the other major protostome group, and they also undergo spiral cleavage. But although the A, B, and C quadrant macromeres also contribute to endoderm in this group, we find no evidence in the literature for the production of a syncytial precursor (e.g., Damen, 1994).

C. Regulation of Macromere Fusion

Granted that the endoderm arises from a syncytial yolk cell (SYC), we then face the question of how that SYC arises. *A priori,* syncytial cells can arise either by karyokinesis without cytokinesis, or by cell fusion as in leech. In some insects, such as *Drosophila,* the syncytial yolk cell arises by nuclear division without cytokinesis. But in others there are initial holoblastic cleavages followed by cell fusion, as in the leech *Helobdella,* and it seems likely that the latter process would be ancestral to the former.

As with any other embryonic cell–cell fusion process, the stepwise fusion of macromeres, teloblasts, and (probably) supernumerary blast cells must be carefully regulated both in terms of cell specificity and in the timing of the fusion process. Having investigated the regulation of the fusion of the A''' and B''' macromeres in *H. robusta,* we find that the process is not autonomous to the fusing cells, but rather requires a signal from D quadrant cells. Both the signaling process and the fusion process become immune to the effects of microinjected ricin A chain many hours before fusion can be detected.

In leech, the SYC ultimately receives contributions of nuclei and cytoplasm from macromeres, teloblasts, and blast cells. Presumably, the mechanism of cell–cell fusion is the same for all the cells contributing to the SYC. But it seems likely that the regulation of the various fusion steps will be more complex, given the very different times and classes of embryonic cells involved.

D. Epiboly

The orchestrated movements of populations of cells are among the most fascinating and least understood aspects of embryogenesis. Epiboly is one dramatic example of such morphogenetic cell movements, and is relatively accessible for analysis because it occurs on the surface of the embryo and involves relatively simple sets of cells. The fact that the same term is applied to processes in animals so highly diverged as leeches and fish begs the question of what, if any-

thing, the two processes have in common beyond the operationally equivalent spreading of one layer of cells over another.

Our investigations of epiboly in glossiphoniid leech embryos are at an early stage. But our electron microscopic studies of the cell–cell contacts lead us to appreciate the important fact (of which we should probably already have been well aware), namely, that the entire surface of the embryo, both the macromeres and the micromere-derived cells, constitutes a *single* epithelium. Thus, contrary to the implications of the commonly used definition of epiboly, there is no "free edge" of the advancing portion of the epithelium. This realization, along with time-lapse video observations (P. Chang, unpublished observations), rules out a notion that otherwise seemed reasonable, namely, that the micromere-derived epithelium spreads by lamellipodial movements at its leading edge, as do epithelia in culture (see Bray, 1992). Now, viewing the whole embryonic surface as a single epithelium, we can view epiboly as comprising two parallel and complementary processes. In one, the micromere-derived portion of the epithelium expands continually during epiboly, due to cell division and cell flattening. This expansion is also accompanied by cell shape changes and rearrangements to accommodate the increase and decrease in the perimeter of the micromere-derived portion of the epithelium as it reaches and then passes the equator of the embryo. In the second process, that portion of the embryonic epithelium derived from the macromeres undergoes a progressive loss of apical surface area, in what we can now visualize as another example of apical contraction of a large, yolk-filled epithelial cell.

This view of epiboly should apply equally to glossiphoniid leeches and teleost fish, such as *Fundulus*, wherein the epithelial nature of the junctions between the yolk cell and the margin of the blastoderm epithelium has been described by Betchaku and Trinkaus (1978). But in some other embryos, epibolic process have been described in which there is a free edge to the advancing epithelium, as in ventral enclosure of the nematode hypodermis (Williams-Masson *et al.*, 1997). We suggest that this modification of epiboly will be seen only in animals that have evolved impermeable egg cases or other protective strategies (e.g., the uterus) so that they can afford the luxury of a partially open embryo. Less well-protected embryos must maintain the integrity of their surface epithelium in order to preserve their internal environment and are thereby constrained to carry out epiboly by the apical constriction process proposed here. This seems likely to be the ancestral condition for metazoan embryos.

Acknowledgments

We thank Bob Goldstein and Ray Keller for helpful discussions. Work presented here is supported by the National Science Foundation.

References

Anderson, D. T. (1973). "Embryology and Phylogeny in Annelids and Arthropods." Pergamon, Oxford.

Astrow, S. H., Holton, B., and Weisblat, D. A. (1987). Centrifugation redistributes factors determining cleavage patterns in leech embryos. *Dev. Biol.* **120,** 270–283.

Backx, P. H., Gao, W. D., Azan-Backx, M. D., and Marban, E. (1994). Mechanism of force inhibition by 2,3-butanedione monoxime in rat cardiac muscle: Roles of [Ca2+]i and cross-bridge kinetics. *J. Physiol.* **476,** 487–500.

Betchaku, T., and Trinkaus, J. P. (1978). Contact relations, surface activity, and cortical microfilaments of marginal cells of the enveloping layer and of the yolk syncytial and yolk cytoplasmic layers of *Fundulus* before and during epiboly. *J. Exp. Zool.* **206,** 381–426.

Boyer, B. C., Henry, J. Q., and Martindale, M. Q. (1996). Dual origins of mesoderm in a basal spiralian: Cell lineage analyses in the polyclad turbellarian *Hoploplana inquilina. Dev. Biol.* **179,** 329–38.

Bray, D. (1992). "Cell Movements." Garland Publ., New York.

Bychowsky, A. (1921). Ueber die Entwicklung der Nephridien von *Clepsine sexoculata* Bergmann. *Rev. Suisse Zool.* **29,** 41–131.

Cramer, L. P., and Mitchison, T. J. (1995). Myosin is involved in postmitotic cell spreading. *J. Cell Biol.* **131,** 179–89.

Damen, P. (1994). Cell-lineage, and specification of developmental fate and dorsoventral organization in the mollusc *Patella vulgata.* Ph.D. Thesis. University of Utrecht, Utrecht, Netherlands.

Desjeux, I. (1995). An investigation into the regulation of segment number in the leech. Ph.D. Thesis. University Medical School, Edinburgh, Scotland, UK.

Desjeux, I., and Price, D. J. (1999). The production and elimination of supernumerary blast cells in the leech embryo. *Dev. Genes Evol.* (in press).

Endo, Y., and Tsurugi, K. (1988). The RNA N-glycosidase activity of ricin A-chain: The characteristics of the enzymatic activity of ricin A-chain with ribosomes and with rRNA. *J. Biol. Chem.* **263,** 8735–8739.

Fernandez, J., and Olea, N. (1982). Embryonic development of glossiphoniid leeches. *In* "Developmental Biology of Freshwater Invertebrates" (F. W. Harrison and R. R. Cowden, eds.), pp. 317–361. Alan R. Liss, New York.

Fernandez, J., and Stent, G. S. (1980). Embryonic development of the glossiphoniid leech *Theromyzon rude*: Structure and development of the germinal bands. *Dev. Biol.* **78,** 407–434.

Freeman, G., and Lundelius, J. W. (1992). Evolutionary implications of the mode of D quadrant specification in coelomates with spiral cleavage. *J. Evol. Biol.* **5,** 205–247.

Goldstein, B., and Freeman, G. (1997). Axis specification in animal development. *BioEssays* **19,** 105–16.

Huang, F. Z., Ramirez-Weber, F. A., and Weisblat, D. A. (1999). In preparation.

Isaksen, D. E. (1997). The identification of a TGF-β class gene and the regulation of endodermal precursor cell fusion in the leech. Ph.D. Thesis. University of California, Berkeley, California.

Isaksen, D. E., Liu, N.-J. L., and Weisblat, D. A. (1999). In preparation.

Ishii, R., and Shimizu, T. (1995). Unequal first cleavage in the *Tubifex* egg: Involvement of a monastral mitotic apparatus. *Dev. Growth Differ.* **37,** 687–701.

Keller, R. E., and Trinkaus, J. P. (1987). Rearrangement of enveloping later cells without disruption of the epithelial permeability barrier as a factor in *Fundulus* epiboly. *Dev. Biol.* **120,** 12–24.

Lans, D., Wedeen, C. J., and Weisblat, D. A. (1993). Cell lineage analysis of the expression of an *engrailed* homolog in leech embryos. *Development* **117,** 857–871.

Liu, N.-J. L., Isaksen, D. E., Smith, C. M., and Weisblat, D. A. (1998). Movements and stepwise fusion of endodermal precursor cells in leech. *Dev. Genes Evol.* **208,** 117–127.

Mohler, W. A., Simske, J. S., Williams-Masson, E. M., Hardin, J. D., and White, J. G. (1998). Dynamics and ultrastructure of developmental cell fusions in the *Caenorhabditis elegans* hypodermis. *Curr. Biol.* **8,** 1087–1090.

Nardelli-Haefliger, D., and Shankland, M. (1993). Lox 10, a member of the NK-2 homeobox gene class, is expressed in a segmental pattern in the endoderm and in the cephalic nervous system of the leech *Helobdella. Development* **118,** 877–892.

Nelson, B. H., and Weisblat, D. A. (1991). Conversion of ectoderm to mesoderm by cytoplasmic extrusion in leech embryos. *Science* **253,** 435–438.

Nelson, B. H., and Weisblat, D. A. (1992). Cytoplasmic and cortical determinants interact to specify ectoderm and mesoderm in the leech embryo. *Development* **115,** 103–115.

Pilon, M., and Weisblat, D. A. (1997). A *nanos* homolog in leech. *Development* **124,** 1771–1780.

Sandig, M., and Dohle, W. (1988). The cleavage pattern in the leech *Theromyzon tessulatum* (Hirudinea, Glossiphoniidae). *J. Morphol.* **196,** 217–252.

Savage, R. M., and Shankland, M. (1997). Identification and characterization of a *hunchback* Orthologue, *Lzf2*, and its expression during leech embryogenesis. *Dev. Biol.* **175,** 205–217.

Schmidt, G. A. (1939). Dégénérescence phylogénétique des modes de développement des organes. *Arch. Zool. Exp. Gen.* **81,** 317–370.

Shankland, M. (1984). Positional determination of supernumerary blast cell death in the leech embryo. *Nature (London)* **307,** 541–543.

Shankland, M. (1998). Anteroposterior pattern formation in the leech embryo. *In* "Cell Lineage and Fate Determination" (S. A. Moody, ed.), pp. 207–224. Academic Press, San Diego.

Shimizu, T. (1996a). Behavior of centrosomes in early *Tubifex* embryos: Asymmetric segregation and mitotic cycle-dependent duplication. *Roux's Arch. Dev. Biol.* **205,** 290–299.

Shimizu, T. (1996b). The first two cleavages in *Tubifex* involve distinct mechanisms to generate asymmetry in mitotic apparatus. *Hydrobiologia* **334,** 269–276.

Smith, C. M. (1994). Developmental fates of micromeres in leech embryos and their roles in morphogenesis. Ph.D. Thesis. University of California, Berkeley, California.

Smith, C. M., and Weisblat, D. A. (1994). Micromere fate maps in leech embryos: Lineage-specific differences in rates of cell proliferation. *Development* **120,** 3427–3438.

Smith, C. M., Lans, D., and Weisblat, D. A. (1996). Cellular mechanisms of epiboly in leech embryos. *Development* **122,** 1885–1894.

Solnica-Krezel, L., and Driever, W. (1994). Microtubule arrays of the zebrafish yolk cell: Organization and function during epiboly. *Development* **120,** 2443–2455.

Stent, G. S., Kristan, W. B., Jr., Torrence, S. A., French, K. A., and Weisblat, D. A. (1992). Development of the leech nervous system. *Int. Rev. Neurobiol.* **33,** 109–193.

Sulston, J. E., Schierenberg, E., White, J. G., and Thomson, J. N. (1983). The embryonic cell lineage of the nematode *Caenorhabditis elegans. Dev. Biol.* **100,** 64–119.

Symes, K., and Weisblat, D. A. (1992). An investigation of the specification of unequal cleavages in leech embryos. *Dev. Biol.* **150,** 203–218.

Trinkaus, J. P. (1984). Mechanism of *Fundulus* epiboly—A current view. *Am. Zool.* **24,** 673–688.

Wedeen, C. J. (1995). Regionalization and segmentation of the leech. *J. Neurobiol.* **27,** 277–293.

Weisblat, D. A. (1999). Cellular origins of bilateral symmetry in glossiphoniid leech embryos. *Hydrobiologia* (in press).

Weisblat, D. A., and Shankland, M. (1985). Cell lineage and segmentation in the leech. *Phil. Trans. R. Soc. Lond. Ser. B* **312,** 39–56.

Weisblat, D. A., Kim, S. Y., and Stent, G. S. (1984). Embryonic origins of cells in the leech *Helobdella triserialis. Dev. Biol.* **104,** 65–85.

Weisblat, D. A., Wedeen, C. J., and Kostriken, R. G. (1994). Evolution of developmental mechanisms: Spatial and temporal modes of rostrocaudal patterning. *Curr. Top. Dev. Biol.* **29,** 101–134.

Weisblat, D. A., Huang, F. Z., and Isaksen, D. E. (1998). Cell fate specification in glossiphoniid leech: Macromeres, micromeres and proteloblasts. *In* "Cell Lineage and Fate Determination" S. A. Moody, ed.), pp. 185–196. Academic Press, San Diego.

Whitman, C. O. (1878). The embryology of Clepsine. *Q. J. Microsc. Sci.* **18,** 215–315.

Williams-Masson, E. M., Malik, A. N., and Hardin, J. (1997). An actin-mediated two-step mechanism is required for ventral enclosure of the *C. elegans* hypodermis. *Development* **124,** 2889–2901.

Wilson, E. B. (1892). The cell lineage of *Nereis. J. Morphol.* **6,** 361–480.

Zackson, S. L. (1984). Cell lineage, cell–cell interaction, and segment formation in the ectoderm of a glossiphoniid leech embryo. *Dev. Biol.* **104,** 143–160.